# Role of iron species in the photo-transformation of phenol in artificial and natural seawater.

Paola Calza*, Cristina Massolino, Ezio Pelizzetti, Claudio Minero

Dipartimento di Chimica Analitica, Università di Torino, via P. Giuria 5, 10125 Torino

**Abstract**

The role played by iron oxides (goethite and akaganeite) and iron(II)/(III) species as photo-sensitizers toward the transformation of organic matter was examined in saline water using phenol as a model molecule. The study was carried out in NaCl 0.7 M solution at pH 8, artificial (ASW) and natural (NSW) seawater, in a device simulating solar light spectrum and intensity. Under illumination phenol decomposition occurs in all the investigated cases. Conversely, dark experiments show that no reaction takes place, implying that phenol transformation is a light-activated process. Following the addition of Fe(II) ions to aerated solutions, Fe(II) is easily oxidized to Fe(III) and hydrogen peroxide is formed. Regardless of the addition of Fe(II) or Fe(III) ions, photo-activated degradation is mediated by Fe(III) species.

Several (and different) hydroxylated and halogenated intermediates were identified. In ASW, akaganeite promotes the formation of *ortho* and *para* chloroderivatives (2- and 4-chlorophenol, 2,4-dichlorophenol and 2,4,6-trichlorophenol), whilst goethite induces the formation of 3-chlorophenol and bromophenols. Conversely, Fe(II) or Fe(III) addition causes the formation of 3- and 4-chlorophenol and 2,3- or 3,4-dichlorophenol. 4-Bromophenol was only identified when irradiating Fe(II) spiked solutions.

Natural seawater sampled in the Gulf of Trieste, Italy, has been spiked with phenol and irradiated. Phenol photo-induced transformation in NSW mediated by natural photosensitizers occurs and leads to the formation of numerous halophenols, condensed products and nitrophenols. When NSW is spiked with phenol and iron oxides, Fe(II) or Fe(III), halophenols production is enhanced. A close analogy exists between Fe(III), Fe(II)/goethite in ASW and NSW products. Different halophenols production in the natural seawater samples depends on Fe(II)/goethite (above all for 3-chlorophenol, 2,3-dichlorophenol and 4-bromophenol formation) and on Fe(III) colloidal species (3-chlorophenol).

**Keywords**: iron, phenol, chlorophenols, photodegradation, seawater

*corresponding author. Phone: +390116707626; fax: +390116707615;
*e-mail: paola.calza@unito.it*

## 1. Introduction

The concentration of total dissolved iron in the oceans ranges from 0.01 to 10 nM, and includes both small soluble Fe species and colloidal forms (Nishioka, et al. 2001; Sarthou, and Jeandel, 2001; de Jong et al, 2007); substantial portion of soluble Fe is present in the colloidal size range (80 to 90 % in near-surface waters) (Wu et al, 2001). Fe(II) in seawater is usually present as complexed species, such as $FeCO_3$ or $FeCl^+$ and, under oxic conditions at the pH of seawater, Fe(II) species are rapidly oxidized to Fe(III) by $O_2$ and $H_2O_2$, as Fe(III) is the thermodynamically stable form of iron in seawater, freshwater and most aqueous systems containing dissolved oxygen. The transformation of dissolved Fe(II) species to particulate Fe(III)oxyhydroxides is central in the cycling of iron in aquatic environments (Stumm and Sulzberger, 1992; Rose and Waite 2002). Particulate Fe(III) oxyhydroxides are formed by oxidation of Fe(II) at the oxic/anoxic boundary in coastal marine waters (Yao and Millero, 1995, Kuma et al. 1998). Possible semiconduction properties of many Fe(III) oxides, oxy-hydroxydes and hydroxides have drawn attention for their role in the natural abiotic transformation of the organic matter (Feng and Nansheng, 2000; Leland and Bard, 1987). In the surficial layer iron oxides could be in the form of goethite (α-FeOOH ), hematite (α-$Fe_2O_3$) and akaganeite (β-FeOOH). These oxides in the presence of oxygen and under illumination could catalyze the oxidation of organic compounds, especially in natural waters and in atmospheric and surface droplets (Kormann et al. 1989)**;** the simultaneous presence of iron species able to act as photo-sensitizers and the high halide concentration could induce organic matter halogenation in seawater. In a previous work, we have assessed the formation of halophenols in water rich of halides in the presence of iron oxides (Calza et al., 2005). Analogously, in the marine ecosystem photosensitized transformations of the organic matter, mediated by metal ions, may occur and produce halogenated species.

Phenol was chosen as a model molecule to simulate organic matter tranformation and, for such, its concentration was similar to that of the natural organic matter content. Phenol photo-induced transformation in seawater proceeds through the formation of a wide range of intermediate compounds, of which most are toxic compounds, including mono and dichlorophenols, nitrophenols, bromophenols and bisphenols (Calza et al., 2008). Because numerous intermediates are formed, the contribution of different photosensitizers are invoked. Possible photosensitized pathways include the sensitization by dissolved organic matter, the direct photolysis of sunlight-absorbing molecules and the reaction with transient species, like OH radicals produced by irradiation of diverse photoactive species (DOM itself, nitrate, nitrite, $H_2O_2$, Fe(III) species) (Boule et al., 2005). At present, scarce investigation is reported for

marine ecosystems on the role of natural photosensitizers and their effect on the possible abiotic transformation of anthropogenic compounds and their degradation products.

The role played by the diverse natural photosensitizing species in the transformation of organic matter in seawater needs attention. This paper focus on the ability of iron species to act as photo-sensitizers toward the phenol transformation. This work is the first of a set on which the link among the natural photosensitizers and the secondary pollutants formed is for the first time evidenced.
The goal is obtained in two steps. Firstly, the experiments were carried out in artificial seawater (ASW). Measures in NaCl 0.7 M solution at pH 8 have also been carried out to evaluate the effect of salinity on the transformation rate and mechanism of phenol photo-induced degradation. The study of the overall process involved the identification and quantification of intermediates and the assessment of hydrogen peroxide formation. Secondly, results achieved in the marine water simulations were compared with those found in the natural seawater samples (NSW).

## 2. EXPERIMENTAL SECTION

### *2.1. Irradiation procedures*

The irradiation experiments were carried out in sealed Pyrex glass cells (46 mm internal diameter), containing 5 ml of the samples. The illumination was performed using a Solarbox with a 1500 watt Xenon lamp equipped with a 340 nm cut-off filter (CO.FO.MEGRA, Milan, Italy) simulating AM1 solar light. Spectroradiometric data for Solarbox is shown in Fig. S1 as supplementary material. The temperature reached during the irradiation was 38° C. Every 24 h during illumination the cells were opened to allow air equilibration.

Phenol photo-induced transformation has been investigated in solutions added with iron oxides (200 $mgL^{-1}$), Fe(II) ($1x10^{-4}$ M) or Fe(III) ($1x10^{-4}$ M) ions at pH 8 in 0.7 M NaCl solution, artificial seawater (ASW) or natural seawater (NSW). Natural seawater (NSW) was sampled in June 2007 in the Gulf of Trieste, northern Adriatic Sea, Italy under the project in acknowledgement (see Table 1 for NSW analysis). Experiments reported below in 3.3. have been performed just after the sampling.

### *2.2. Analytical determinations*

The disappearance of phenol and formation of intermediates were followed using a HPLC system (Merck-Hitachi L-6200 pumps), equipped with a Rheodyne injector, a RP C18 column (Lichrochart, Merck, 12.5 cm x 0.4 cm, 5 μm packing) and a UV-Vis detector (Merck Hitachi L-4200). The disappearance of phenol was followed at 220 nm, using 30% acetonitrile and 70%

phosphate buffer (1 x $10^{-2}$ M) at pH 2.8 and at a flow rate of 1 ml/min (detection limit for phenol 0.1 ppm). The intermediates formed along with the phenol photo-induced transformation have been identified by HPLC, through a comparison with standard solutions, and confirmed by GC/MS analysis.

A GC/MS Agilent 6890, series II, equipped with a 5% phenylmethylpolysiloxane column Agilent HP-5; 30 m x 0.25 mm was used. Other conditions have been described elsewhere (Calza et al., 2008).

Iron (II)/(III) and $H_2O_2$ concentrations have been measured using UV-Vis spectrophotometry (Varian Cary 100). Hydrogen peroxide was quantified by the peroxidase-catalysed oxidation of phenol/4-aminoantipyrine protocol (Frew et al. 1983). Measurements were made at 505 nm.

Fe(II) formation has been followed through colorimetry, complexing $Fe^{2+}$ with 1,10-phenanthroline (Calza et al. 2008). The absorbance of the complex $[(C_{12}H_{18}N_2)_3Fe]^{2+}$ was measured at 511 nm. Due to the LOD determined for Fe(II) and Fe(III), (1x$10^{-6}$ M) concentrations higher than in natural seawater have been utilized in the experiments.

*2.3. Material and reagents*

Goethite (α-FeOOH) and akaganeite (β-FeOOH) have been synthesized following literature reference (Bakoyannakis et al. 2003).

Phenol, catechol, 1,4-benzoquinone, 1,3,5-trihydroxybenzene, 2-chlorophenol, 3-chlorophenol, 4-chlorophenol, 2-bromophenol, 4-bromophenol, 2,6-dichlorophenol, 3,5-dichlorophenol, 3,4-dichlorophenol, 2,2'-bisphenol, 4,4'-bisphenol, Fe(III) perchlorate, 4-aminoantipyrine and hydroquinone were all purchased from Aldrich and were used as received. 2,3-Dichlorophenol, 2,4-dichlorophenol, 2,5-dichlorophenol were purchased from Fluka, $FeSO_4$ from Carlo Erba and acetonitrile from Scharlau (AC033 Supergradient HPLC grade).

Eluents have been prepared in MilliQ water and degassed before utilization. Artificial seawater (ASW) has been prepared in MilliQ water containing the salts in the indicated amounts summarized in Table 2 (Kester et al. 1967). The pH was adjusted by addition of NaOH 0.1 M.

## 3. Results and discussion

Iron(II) and iron(III) speciation is a function of the pH (Santana-Casiano et al. 2006), so that phenol photo-degradation could be induced by different species. The transformation process could be mediated by aqueous species or could occur at the water/solid interface of precipitates. The

equilibrium among the different iron species could be (or not) easily reached. Therefore, when Fe(II)/Fe(III) species are initially added, preliminary experiments have been performed to assess the rate of iron species transformation. Once these details were known, the role of chloride and carbonate ions on the phenol transformation rate was also evaluated.

### *3.1. Phenol photo-induced disappearance in NaCl and ASW*

#### *3.1.1. Iron oxides*

The study of the phenol photoinduced transformation as a function of the pH and chloride concentration was preliminary done for goethite and akaganeite (supplementary data S2-S6). Generally, chloride concentration depresses the rate, whilst the dependence on pH is more complex. In this paper it will only be discussed results at pH 8. Experiments have been performed in NaCl 0.7 M solution or ASW and the phenol disappearance rates under the different experimental conditions are shown in Table 3. In both media, akaganeite is the more efficient catalyst, while goethite shows the lowest rate. A preliminary explanation could be attributed to the different oxidation potentials of valence band holes, approximately accordingly to $E^{o}_{VB}$ potential for goethite (2.3 eV), and akaganeite (2.5 eV). A comparison between the chloride enriched solution and ASW shows that in all cases the addition of other salts (above all carbonate ions) scarcely influences phenol degradation rates. Although rates are low, accordingly to Leland and Bard (1987), it is well-known that phenol photo-induced transformation in the presence of semiconductor oxides occurs through the formation of hydroxy derivatives.

Conduction band electrons ($e_{CB}^{-}$) at the iron oxide surface could lead to the catalyst photo-dissolution, with subsequent reduction of Fe(III) by photoelectrons. Under illumination the formation of Fe(II) from iron oxides occurs (see Fig. S2, S4-S6, supplementary material). A correlation exists between the amount of formed Fe(II) and the phenol disappearance rate. Akaganeite leads to the highest degradation rate (see Table 3) and the largest transient Fe(II) concentration (7 $mgL^{-1}$), while the lowest rate and Fe(II) concentrations were observed for goethite.

#### *3.1.2. Fe(II)/Fe(III)*

The irradiation of phenol solution added with Fe(II) or Fe(III) has been carried out on: 1) filtered or unfiltered solutions, aimed to discriminate the role of the precipitate iron on the process. At pH>6,

Fe(III) is chiefly in the insoluble $Fe(OH)_3$ (ferrihydrite) form, so that the photo-degradation process could occur at the water/solid interface (Calza, et al. 2005) as already observed in seawater (Byrne, and Kester, 1976, Kuma, et al. 1992 and 1996); 2) stirred (for 96h) or unstirred solutions, in order to evaluate if the equilibrium among the different species is easily (or not) reached.

The phenol disappearance rates, measured under the diverse experimental conditions, are also reported in Table 3. No reaction takes place in the dark, neither with Fe(II) nor with Fe(III), while under illumination the phenol transformation occurs in all the considered cases. Phenol is very slowly transformed (after 64 h of irradiation only 20% of the initial compound has been degraded) and only little differences among the investigated cases exist.

Taking into accounts these results, some implications come up:

(1) no difference arises from phenol rates under stirred (96h before illumination) or unstirred solutions, implying that the chemical equilibrium among the diverse iron species is quickly reached;

(2) no significant variation is evidenced between the filtered and unfiltered samples. Owing to these data, it can be concluded that the larger solid phase particles do not influence the kinetic of the process. Since the precipitate formed at pH 8 does not to modify the iron(II)/(III) photo-activity, phenol photo-transformation should then be chiefly induced by colloidal species.

It is worth noting that the phenol disappearance rates do not show remarkable difference when Fe(II) or Fe(III) have been initially added (see Table 3). Measurement of iron(II) in solution had shown that, when Fe(II) is the starting species, it is rapidly oxidized to Fe(III). In few minutes before illumination almost 50% of the Fe(II) was oxidized to Fe(III). It has to be underlined that under irradiation Fe(II) can be oxidized to goethite (Chen et al. 2007), so that the close analogy between the Fe(II) and Fe(III) degradation profiles suggests an involvement of Fe(III) colloidal species rather than Fe(II) species in photo-assisted phenol degradation.

The understanding of what occurs in colloidal phase could be extrapolated from the equilibrium in solution, due to the analogies existing between colloidal and aqueous phases (Stumm and Sulzberger, 1992).

In Fe(II) spiked solution, its rapid oxidation should be due to dissolved oxygen as a result of reactions 1-2 (Miller et al. 1995).

$$Fe^{2+} + O_2 \rightarrow Fe^{3+} + \cdot O_2^- \qquad k = 13\ (M^{-1}\ sec^{-1}) \qquad (1)$$

$$Fe^{2+} + \cdot O_2^- + 2H^+ \rightarrow Fe^{3+} + H_2O_2 \qquad k = 1.0 \times 10^7\ (M^{-1}\ sec^{-1}) \qquad (2)$$

$$2 \cdot O_2^- + 2H^+ \rightarrow H_2O_2 + O_2 \qquad (3)$$

According to these equations, hydrogen peroxide formation is expected. $H_2O_2$ formation was monitored as a function of irradiation and is shown in Figure 1A. Part of the $H_2O_2$ is already formed in the dark before the experiment begins, but its formation is enhanced under illumination. The production of hydrogen peroxide reveals that the Haber-Weiss mechanism occurs (Santana-Casiano et al. 2005) (reactions 1-6), with the consequent production of hydroxyl radicals able to promote the phenol disappearance according to reaction 8 (Buxton et al. 1988).

$$Fe(II) + {}^{\bullet}HO_2 + H^+ \rightarrow Fe(III) + H_2O_2 \qquad k_1 \qquad (4)$$

$$Fe(II) + H_2O_2 \rightarrow Fe(III) + \cdot OH + OH^- \qquad k_2 \qquad (5)$$

$$Fe(II) + \cdot OH \rightarrow Fe(III) + OH^- \qquad k_3 \qquad (6)$$

$$\cdot OH + H_2O_2 \rightarrow {}^{\bullet}HO_2 + H_2O \qquad k_4 \qquad (7)$$

$$\Phi\text{-}OH + \cdot OH \rightarrow \text{products (see below)} \qquad k_5 \qquad (8)$$

where Φ-OH is phenol. Bautista et al 2008 report a $k_2$=76 $M^{-1}$ $sec^{-1}$, while the kinetic constants calculated by Santana-Casiano et al. 2005 in sea water, at pH 8 and ionic strength 0.7 M are higher ($k_1$=1.2x10$^6$ ($M^{-1}$ $sec^{-1}$), $k_2$= 3.1x10$^4$ ($M^{-1}$ $sec^{-1}$) $k_3$= 5.0x10$^8$ ($M^{-1}$ $sec^{-1}$), $k_4$= 2.7x10$^7$($M^{-1}$ $sec^{-1}$) $k_5$=1.4x10$^{10}$($M^{-1}sec^{-1}$)).

Back reactions have also to be considered, where Fe(III) reacts with $\cdot O_2^-$ (eq. 9) (Rose and Waite 2002, King, et al. 1995), and Fe(III) is hydrolyzed to form insoluble $Fe(OH)_3$ (eq. 10) (Rose and Waite 2002).

$$Fe(III) + \cdot O_2^- \rightarrow Fe(II) + O_2 \qquad k= 1.5x10^8\ (M^{-1}\ sec^{-1}) \quad (9)$$

$$Fe(III) + 3OH^- \rightarrow Fe(OH)_{3(s)} \qquad k= 2.5x10^4\ (M^{-1}sec^{-1}) \quad (10)$$

When Fe(III) is the starting species, under UV light irradiation colloidal Fe(III) hydroxy-complexes undergo photochemical reduction to Fe(II) (Joseph et al. 2001, Baxendale et al., 1955) and the ·OH radical formation can be realized accordingly to the reaction 11 (Feng and Nansheng, 2000):

$$Fe\text{-}(OH)^{2+} \xrightarrow{h\nu} Fe^{2+} + \cdot OH \qquad (11)$$

Also the formation of hydroquinone-like intermediates could be an alternative route for Fe(III) reduction to Fe(II) (Du et al., 2006).

Iron(II) formation was in effect observed, at concentrations ranging from $2x10^{-6}$ M to $5x10^{-6}$ M. As a consequence of Fe(III) reduction, hydrogen peroxide formation is achieved (see Figure 1B). The formation of ·OH radicals will support both hydrogen peroxide formation, as a result of reactions 3-4, and phenol transformation.

*3.1.3. Role of salts on the disappearance rates*

The phenol disapperance rates is scarcely influenced by the iron speciation with diverse salts, above all carbonate species (see Table 3 and Figure S7 supplementary material). This is in agreement with the active role played by colloidal Fe(III) species, that are scarcely influenced by iron speciation. Closer inspection of Table 3 reveals that, even if phenol disappearance rates are similar in the diverse experimental conditions, in ASW rates are slightly lowered, due to the speciation as $Fe(CO)_3)_2^{2-}$ (King and Farlow 2000). In addition, the superoxide $\cdot O_2^-$ and ·OH radicals can act as oxidants for other reduced compounds, i.e. $Cl^-$ and $HCO_3^-$ (McElroy, 1990, Emmenegger et al. 1998, Petasne and Zika, 1987). These newly generated radicals can play the role of ·OH radical in the reaction (6), although these radicals are less reactive than ·OH (Miller et al. 1995, Emmenegger et al. 1998).

$HCO_3^-$ can form the $CO_3\cdot^-$ radical, according to reaction (12), then producing a new radical species able to react with phenol (reaction 13) but with a constant rate lower than ·OH radical (Neta, et al. 1988).

$$\cdot OH + HCO_3^- \rightarrow H_2O + CO_3\cdot^- \qquad k = 8.5x10^6\ (M^{-1}\ sec^{-1})\ (12)$$

$$\Phi\text{-}OH + CO_3\cdot^- \rightarrow C_6H_5O\cdot + HCO_3^- \qquad k = 4.9\ x10^6\ (M^{-1}\ sec^{-1})(13)$$

The presence of bicarbonate will then induce a decrease in the phenol disappearance rate. Conversely and surprisingly, the presence or absence of chloride ions does not affect the phenol disappearance rate, as already reported by King et al. (1993) (see Table 3).

By considering the hydrogen peroxide evolution (see Figure 1), $H_2O_2$ maximum concentration is $1x10^{-5}$ M, lowered to $5x10^{-6}$ M in ASW water. This effect is most likely due to scavenging of ·OH radicals by the carbonate ions, according to reaction 12.

***3.2. Intermediate compounds in NaCl and ASW***

*3.2.1. Iron oxides*

Following the mechanism described in 3.1.1, the hydroxy-phenols formation is expected (Santana-Casiano et al. 2006, King, et al., 1993, Pelizzetti et al. 1990). Other radical species could also act as oxidative agents, such as $O_2{\cdot}^-$ and $HO_2{\cdot}$, produced according to reactions (1) or (7) .

Looking closer at iron oxides addition in ASW, in all cases hydroquinone is the main intermediate, then easily transformed into 1,4-benzoquinone (see Figure 2-3 for temporal evolution, Figure 4 for their maxima amount and Figure S8-S14 for data at different pHs in the presence of NaCl). A secondary pathway leads to the formation of several condensed products, similarly to what was observed in previous studies on $TiO_2$ (Azavedo et al. 2004). The dimerization reaction would hardly occur in homogeneous solution due to extremely low concentrations of transient radicals. The formation of condensed products at concentrations comparable to that of the starting precursor (phenol) indicates that this reaction, and consequently all the reactions that involve transient radicals, occurs at the surface of mineral particles where reagents are compartmentalized. Local concentrations can be deeply different from bulk concentration.

The hydroxylated and condensed products could be formed through the well known mechanism of radical attack to the aromatic ring. Firstly, an ·OH radical addition could occur at *ortho* (or *para*) positions. Through a further involvement of a superoxide radical anion, the formation of catechol and hydroquinone is realized. Conversely, the formation of hydroquinone has been postulated as an intermediate step to account for the occurrence of 1,4-benzoquinone (Boule, et al., 1999). The formation of dimers, like bisphenols, passes through the phenoxyl radical dimerization, in equilibrium with its tautomeric form.

In addition to hydroxylation mechanism, the organic matter chlorination could also take place (Figure S10 and S12-S13). The chloro radical formation occurs according to reactions 14-17 and involves chloride oxidation mediated by ·OH radicals (Buxton et al. 1998) (eq. 14-15):

$$Cl^- + {\cdot}OH \rightarrow ClOH^-{\cdot} \quad (14)$$

$$ClOH{\cdot}^- + H^+ \rightarrow Cl{\cdot} + H_2O \quad (15)$$

$$Cl{\cdot} + Cl^- \rightarrow Cl_2{\cdot}^- \quad (16)$$

$$Cl_2{\cdot}^- + {\cdot}OH \rightarrow HOCl + Cl^- \quad (17)$$

In chloride rich water, chlorine is mainly as $Cl_2{\cdot}^-$ radical (Buxton et al. 1998), produced through the reaction 16. This species is responsible for the attack to the organics with the formation of the

chlorinated species. Analogously, bromo radicals could be formed and lead to the formation of bromophenols (Vione et al. 2008).

Experiments performed in NaCl solution (pH 8) showed a slight formation of chloroderivatives. Akaganeite induces the formation of 2-chlorophenol (80 ppb), while no chloroderivatives are observed with goethite (see Figure S12 at pH 8).

Conversely, in ASW solution the chlorination reaction easily occurs and several chlorinated compounds are formed (see Figures 2, 3). Different iron oxides produce distinct chloroderivatives distribution. Akaganeite induces the formation of 2- and 4-chlorophenol (CP), 2,4-dichlorophenol (DP) and 2,4,6-trichlorophenol (TP), while goethite promotes the formation of 2- and 4-bromophenol (BrP), 2- and 3-chlorophenol.

Two different pathways for phenol chlorination are proposed, based on two diverse oxidation mechanisms: the ·H abstraction (mechanism 1) or the ·OH addition (mechanism 2), which is prevalent when the oxidant is ·OH radical (Albarràn et al. 2002) (see Scheme 1). In the first case, after ·H abstraction (by any agent capable of H-abstraction, like OH or $Cl_2^-$ radicals, or capable of electron-transfer from deprotonated phenoxide, or by OH addition followed by $H_2O$ loss), the further addition of $Cl_2\cdot^-$ leads to the formation of "classical" *ortho* and *para* orientated monochloro-derivatives, in agreement with literature data (Azavedo et al. 2004). In the case of chlorophenols, taking into account that hydroxyl function is *ortho*, *para* orienting and activating and that –Cl is *ortho*/ *para* orienting and deactivating, a further ·H abstraction is possible in *o*, *p*-position with respect to the phenolic hydroxyl. Dichloro derivatives (2,4-DP and 2,6-DP) should then be formed following a second step of mechanism "type 1" through a further $Cl_2\cdot^-$ radical attack, as shown later in Scheme 2.

A different pathway (mechanism 2) is invoked to justify the observed formation of *meta* derivatives. In this second type of mechanism, the formation of the *meta* halogenated derivatives could take place through an ·OH radical mediated attack: an initial ·OH radical addition occurs (on *para* or *ortho* position) that allows the entrance of a $Cl_2^-\cdot$ radical in *meta* position, followed by a release of water. This mechanism is also operating when some positions on the aromatic ring are occupied by chlorine. The general rule is that there is addition of chlorine to the adjacent carbon (α-carbon) to the position where OH radical attack is allowed if there is a C-H bond.

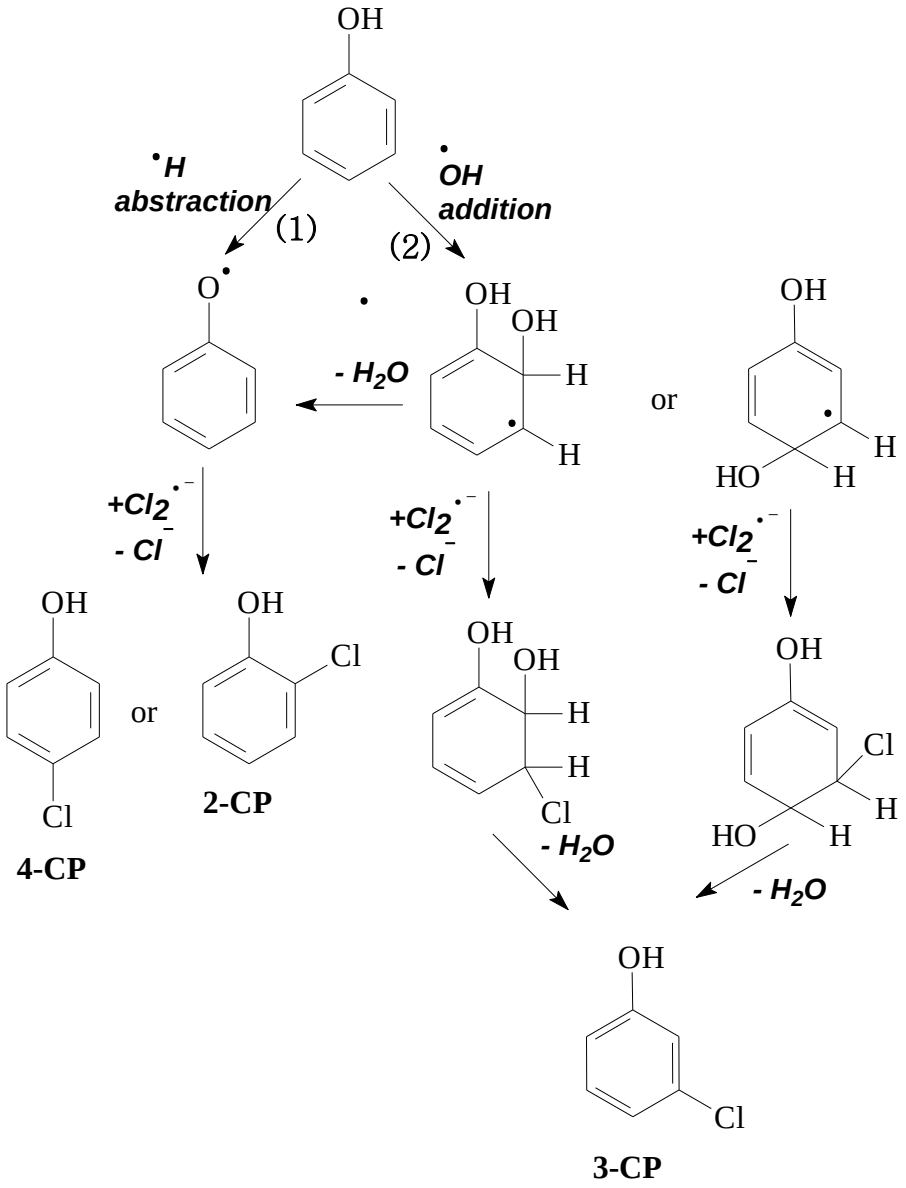


**Scheme 1.** Proposed mechanisms for the formation of monochlorophenols

A further step of mechanism (2) will lead to the formation of 3,5-DP, as described in Scheme 2. A sequence of mechanism 1 and 2 leads to 3,4-, 2,3- and 2,5-DP formation. This mechanism could explain the formation of diverse intermediates but is silent on why in the presence of akaganeite or goethite preferential ·H abstraction or ·OH addition could occur. Bromophenols are also observed. In this case only mechanism 1 occurs and only regioselective derivatives (2- and 4-BrP) are formed. This is probably due to the easier formation of $\cdot Br/Br_2\cdot^-$ couple (Calza et al. 2005) that favours bromide addition over OH addition to the aromatic ring.

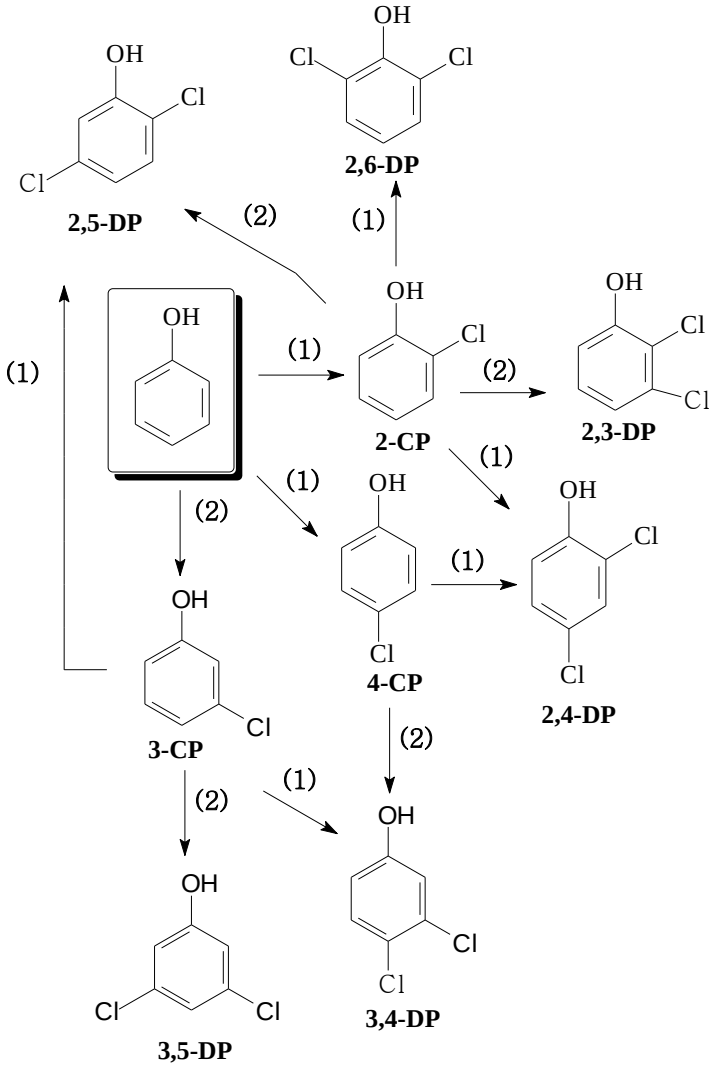


**Scheme 2.** Proposed mechanism for the formation of chloro and dichloro-derivatives; in parenthesis the type of mechanism involved.

*3.2.2. Fe(II)/Fe(III)*

Addition of Fe(II)/Fe(III) produces similar intermediates and temporal profiles for all the stirred and filtered solutions, underlining that size of formed particulate neither influenced the phenol disappearance rate or its transformation mechanism. However, experiments carried out on filtered solution showed that removal of the macroscopic solid phase (>0.5 μm) slightly lowers the intermediates concentration, above all for halogenated compounds. It suggests that both for (amorphous) colloidal phase (Fe(II)/Fe(III) addition) and larger and crystalline phases the basic chemistry does not change. This implies that key species are surficial hydroxylated species. A semiconductor-like effect of crystalline phase can increase the efficiency.

If the degradation pathway effectively proceeds through the ·OH radicals production, according to reaction 11 (where $Fe(OH)^{2+}$ can be assumed as surficial iron species into the oxide

matrix) hydroxyl derivatives are expected (Faust 1999). Experimentally, hydroquinone, resorcinol, 4,4'-bisphenol, 2,2'-bisphenol and 1,4-benzoquinone were identified, as shown in Figures S15-16 for temporal evolution and Figure 4 for maxima concentrations, suggesting that an oxidation mechanism is operating.

However, the mechanism depends on the amount of Fe(II) and Fe(III) actually present. When Fe(II) is initially added (see Figure 4 and S15), hydroquinone is the main intermediate, catechol is absent and several differences arise for other hydroxyl derivatives. In ASW only hydroquinone and 1,4-benzoquinone were identified, while in NaCl solution, resorcinol and *para* condensed derivatives were observed.

When Fe(III) is the starting species (see Figure 4 and S16), hydroquinone is still one of the main intermediates, while catechol and resorcinol are always absent; in NaCl solution 1,4-benzoquinone is also formed, in a close analogy with the cases with iron oxides.

*Halophenols formation*

Several chloro and dichloro derivatives are also formed. Chlorination of organic matter could be justified by assuming the chloro radical formation through ·OH-mediated oxidation (see reactions 14-17). An alternative route for chloro radical formation involves $FeCl^{2+}$ species photo-dissociation but only occurs at pH<5 (Millero et al. 1998).A competitive reaction of $Cl_2{\cdot}^-$ radical (reaction 18) with Fe(II) should also occur, subtracting Cl radicals (Buxton et al. 1998).

$$Fe^{2+} + Cl_2{\cdot}^- \rightarrow Fe^{3+} + 2Cl^- \qquad (18)$$

Interestingly, when considering the case of the solution spiked with Fe(II), 3-CP is formed at similar amount in both NaCl and ASW media. Thus, its formation is not influenced by the presence of diverse salts. The prevalent formation of meta chloroderivatives was already observed from bisphenol in NaCl solution (Liu et al. 2009). 2-CP and 2,3-DP (NaCl) or 2,3-DP and 4-BrP (ASW) formation also occurs.

In the experiments performed with added Fe(III), 3- and 4-CP and 3,4-DP are predominantly formed in both NaCl and ASW solution. In addition, 2-CP formation only occurs in NaCl solution. Since measurement of iron(II) in solution had shown that it is rapidly oxidized to Fe(III), the existence of two diverse halophenols distribution is consistent with the proposed mechanisms 1 and 2 when reaction (11) is the source for •OH radicals and, subsequently, •Cl is formed through reaction 14 and 15. Addition of Fe(II), which is partially oxidized to Fe(III), leads to the species $Fe(OH)_2^+$ and, after photoabsorption, to •OH radicals. These are scavenged by Fe(II) and $Cl^-$. Under

these conditions, mechanism 2 is operating forming 3-CP. Direct addition of Fe(III) increases the •OH/•Cl ratio, leading to mechanism 1 and forming 4-CP These reactions are of course at the colloid interface. Fe(III) formed from Fe(II) oxidation precipitates as goethite (Joseph et al. 2001), a phase probably different from that generated by Fe(III) hydrolysis. This suggestion is in agreement with what was before described for iron oxides, where different oxides promote the formation of diverse chloroderivatives (see section 3.2.1).

These results imply that the preferential formation of different halo derivatives isomers can be a way to discriminate the iron(II)/(III) sources. It is of environmental relevance that, according to the genesis of precipitates, different isomers are observed. For example, under anoxic condition (i.e. sediments) iron(II) could be released; when this is oxidized to Fe(III), the case is similar to addition of Fe(II) above. It precipitates in a form that differs from that formed when Fe(III) precipitates in estuarine waters or is supplied by atmospheric dust (de Jong, 2007). It is then expected that different haloderivatives are formed depending on the iron genesis.

### *3.3. Natural seawater*

NSW was spiked with phenol and irradiated as described above. Upon light exposure, the phenol photo-transformation occurs ($t_{1/2}$ =8 days, k= $1.4x10^{-8}$ $min^{-1}$) and leads to the formation of numerous intermediates (Calza et al, 2008), whose maxima concentrations are shown in Figure 5.

Phenol disappearance rate increases when NSW is added with iron species (rate constant ranging from $2.4x10^{-8}$ $min^{-1}$ (Fe(II)) to $3.2x10^{-8}$ $min^{-1}$ (akaganeite)). In all cases the disappearance rates calculated in NSW are higher than those in ASW experiments (see Table 3 and Figure S7 for disappearance profiles). This could be attributed to the existence of other photosensitizers, above all humic and fulvic acids that, following UV-vis absorption, lead to a higher ·OH radicals production. Reduction of Fe(III) to Fe(II) is favoured by the presence of humic acids, thanks to the formation of photochemically-active Fe(III)-organic complexes (Spokes et al. 1995).

In NSW, the formation of hydroxyderivatives (1,4-benzoquinone, resorcinol), three chlorophenol isomers, 2,3-DP, 2- and 4-BrP, 2- and 4-nitrophenol, and several condensed products (2 and 4-phenoxyphenol, 2,2'-, 4,4'- and 2,4-bisphenol) was observed.

NSW has then be spiked with iron oxides (200 $mgL^{-1}$), Fe(II) or Fe(III) $1x10^{-4}$ M and numerous intermediates are formed (see Figures S17-S20 for temporal profiles and Figure 5 for maxima concentration plots). By comparing NSW with NSW spiked with iron species solutions, several considerations come up: condensed products and hydroxyderivatives are formed at similar amount, nitroderivatives maxima concentration are lowered and the role of iron species to induce

halogenation is confirmed. Obviously, nitroderivatives are only observed in NSW since ASW does not contain inorganic nitrogen. A large variety of condensed compounds is formed in NSW and 4-phenoxyphenol is mainly produced, while in ASW 2,2'-bisphenol is prevalently formed.

Interesting differences for halophenols distribution comes up. The peculiar diversity already shown in ASW added with the diverse iron species are still maintained in NSW (Figure 5). NSW spiked with goethite shows an enhanced formation of 4-BrP and 3-CP, while the formation of other haloderivatives is suppressed. 2,6-DP is only formed in NSW spiked with akaganeite. The concentration of other halocompounds still remains the same.

Both Fe(II) and Fe(III) addition to NSW induces inhibition in hydroxy derivatives formation, while the profiles for halophenols formation, above all bromophenols, are strongly modified. By considering the NSW added with Fe(III), 3-CP and 2-BrP concentration are enhanced; Fe(III) addition also induces the formation of 3,4-DP, not detected in NSW, but observed in ASW. In NSW spiked with Fe(II), the formation of 3-CP and bromophenols is strongly increased. Interestingly, the formation of 2,3-DP only occurs with Fe(II). Thus, the Fe(II) species induce the formation also in NSW of the same halophenols described in ASW medium with goethite. The analogies between Fe(II)/goethite and NSW products are remarkable. Looking closer at the bromophenols, with goethite and Fe(II) 4-BrP is more easily formed. The ratio 4-BrP: 2-BrP is 4:1 with added Fe(II) and 2-BrP was not detected with goethite, in a close analogy with NSW, where 2-BrP is only formed at traces amount. In conclusions, the ability to produce halophenols in the natural seawater sample should be linked to Fe(II)/goethite (above all for 3-CP, 2,3-DP and 4-BrP formation) and Fe(III) colloidal species (3-CP).

## 4. Conclusions

Irradiation of natural seawater added with phenol and iron species has provided the enhanced formation of several halophenols, suggesting a central role played by iron species on the phenol halogenation in marine water.

All the discussed results are consistent with the occurrence of two types of mechanisms explaining the formation of ortho/para or meta chloroderivatives. Different oxides provide different chlorinated intermediate products, due to the different specific reaction rate constants of various processes (i.e. photolysis, Fenton and complexation) for the diverse iron oxides. These results suggest that the formation of different chloro derivatives isomers should depend on the

environmental iron genesis. This work supports also the need for specific studies focused on kinetic processes involved at the surface of iron oxide.

**Acknowledgments**

Financial support of Ministero dell'Istruzione, Università e Ricerca through FIRB contract n° RBAU01HLFX is kindly acknowledged.

**References**

Albarràn, G.; Schuler, R.H. Micellar electrophoretic capillary chromatographic analysis of the products produced in the radiolytic oxidation of toluene and phenol Rad. Phys. Chem., 2002; 63: 661-663

Azavedo, E.B.; Neto, F.R.D.; Dezotti, M. $TiO_2$-photocatalyzed degradation of phenol in saline media: lumped kinetics, intermediates and acute toxicity. Appl. Catal. B- Environ., 2004; 54(3): 165-173

Bakoyannakis, D.N.; Deliyanni, E.A.; Zouboulis, A.I.; Matis, K.A.; Nalbandian, L.; Kehagias, Th.; Akaganeite and goethite-type nanocrystals: synthesis and characterization Micropor. Mesopor. Mater. 2003; 59: 35–42

Bautista, P; Mohedano, AF; Casas JA, Zazo, JA; Rodriguez, JJ; An overview of the application of Fenton oxidation to industrial wastewaters treatment, J. Chem. Technol. Biotechnol. 2008; 83: 1323-1338

Baxendale, J.H.; Magee, J. The photochemical oxidation of benzene in aqueous solution by ferric ion. Trans. Faraday Soc., 1955; 51: 205-213

Boule, P.; Bolte, M.; Richard C., The handbook of environmental chemistry, *Vol. 2*, P. Boule ed., Springer, Berlin, 1999**,** 181-215

Boule P, Bahnemann DW, Robertson DW, Robertson PKJ, The Handbook of Environmental Chemistry, Springer ed., Berlin, 2005.

Buxton, G.V.; Greenstock, C.L.; Helman, W.P.; Ross, A.B. J. Phys. Chem. Ref. Data, 1988; 17(2): 513-886

Buxton, G.V.; Bydder, M.; Salmon, G.A. Reactivity of chlorine atoms in aqueous solution - Part 1 The equilibrium Cl-center dot+Cl-reversible arrow $Cl^-_2$(center dot-). J. Chem. Soc., Faraday *Trans*., 1998, 94(5), 653-657

Byrne, R.H.; Kester, D.R., Solubility of hydrous ferric oxide and iron speciation in seawater. Mar. Chem.1976; 4: 255-274

Calza, P.; Maurino, V.; Minero, C.; Pelizzetti, E.; Sega, M.; Vincenti, M. Photoinduced halophenol formation in the presence of iron(III) species or cadmium sulfide. J. Photochem. Photobiol. A: Chem. 2005, 170, 61-67

Calza P., Massolino C., Pelizzetti E., Minero C., Solar driven production of toxic halogenated and nitroaromatic compounds in natural seawater, Sci. Tot. Environ. 2008; 398 (1-3): 196-202

Chen, R.; Chen, H.; Wei, Y.; Hou, D. Photocatalytic oxidation of $Fe(OH)_2$ suspension with visible light irradiation, J. Phys. Chem. C, 2007; 111: 16453-16459

de Jong, J.T.M.; Boyè, M; Gelado-Caballero, M.D.; Timmermans, K.R.; Veldhuis, M.J.W.; Nolting, R.F.; van der Berg, C.M.G., de Baar, H.J.; Inputs of iron, manganese and aluminium to surface waters of the Northeast Atlantic Ocean and the European continental shelf, Mar. Chem., 2007; 107: 120-142

Du, Y.; Zhou, M. ; Lei, L. Role of intermediates in the degradation of phenolic compounds by Fenton-like process. J. Hazard. Mat. B, 2006; 136: 859-865

Emmenegger, L.; King, D.W.; Sigg, L.; Sulzberger, B. Oxidation kinetics of Fe(II) in a eutrophic Swiss lake. Environ. Sci. Technol. 1998; 32: 2990-2996

Faust, B.C. The Handbook of Environmental Chemistry, 2 Part L, 1999,103-122

Feng, W.; Nansheng, D. Photochemistry of hydrolytic iron(III) species and photoinduced degradation of organic compounds. A minireview. Chemosphere, 2000; 41: 1137-1147

Frew, J.E.; Jones, P.; Scholes, G.; Spectrophotometric determination of hydrogen peroxide and organic hydroperoxides at low concentrations in aqueous solution Anal. Chim. Acta, 1983; 155: 139-150

Joseph, J.M.; Varghese, R.; Aravindakumar, C.T. Photoproduction of hydroxyl radicals from Fe(III)-hydroxy complex: a quantitative assessment. J. Photochem. Photobiol. A: Chem, 2001; 146: 67–73

Kester; D.R.; Duedall, I.W.; Connors, D.N.; Pytkowicz, R.M. Preparation of artificial seawater. Limnol. Oceanogr. 1967; 12 (1): 176-179

King, D.W.; Aldrich, R.A.; Charnecky, S.E. Photochemical redox cycling of iron in NaCl solutions. Mar. Chem., 1993; 44: 105-120

King, D.W.; Lounsbury, H.A.; Millero, F.J. Rates and mechanism of Fe(II) oxidation at nanomolar total iron concentration. Environ. Sci. Technol. 1995; 29: 818-824

King, D.W.; Farlow, R. Role of carbonate speciation on the oxidation of Fe(II) by $H_2O_2$. Mar. Chem., 2000; 70: 201-209

Kormann, C.; Bahnemann, D.W.; Hoffmann, M.R.; Environmental photochemistry: is iron oxide (hematite) an active photocatalyst? A comparative study: α-$Fe_2O_3$, ZnO, $TiO_2$, *J.* Photochem. Photobiol. A: Chem. 1989; 48: 161-169

Kuma, K.; Nakabayashi, S.; Suzuki, Y.; Matsunaga, K. Dissolution rate and solubility of colloidal hydrous ferric oxide in seawater. Mar. Chem., 1992; 38: 133-143

Kuma, K.; Nishioka, J.; Matsunaga, K. Controls on iron(III) hydroxide solubility in seawater. The influence of pH and natural organic chelators. Limnol. Oceanogr. 1996; 41: 396-407

Kuma, K.; Katsumoto, A.; Kawakami, H.; Takatori, F.; Matsunaga, K. Spatial variability of Fe(III) hydroxide solubility in the water column of the northern North Pacific ocean. Deep Sea Res. 1998; 45: 91-113

Leland, J.K.; Bard, A.J. Photochemistry of Colloidal Semiconducting Iron Oxide Polymorphs J. Phys. Chem. 1987; 91: 5076-5083

Liu, H.; Zhao, H.; Quan, X.; Zhang, Y.; Chen, S.; Formation of chlorinated intermediate from bisphenol A in surface saline water under simulated solar light irradiation, Environ. Sci. Technol. 2009; 43: 7712-7717

McElroy, W. A laser photolysis study of the reaction of $SO_4^-$ with $Cl^-$ and the subsequent decay of $Cl_2^-$ in aqueous medium. J. Phys. Chem., 1990; 94: 2435-2441

Miller, W.L.; King, D.W.; Lin, J.; Kester, D.R. Photochemical redox cycling of iron in coastal seawater. Mar. Chem. 1995; 50: 63-77

Millero, F.J. Solubility of Fe(III) in seawater Earth Planet. Sci. Lett. 1998; 154: 323-329

Neta, P.; Huie, R.E.; Ross, A.B. J. Phys. Chem. Ref. Data, 1988; 17(3): 1027-1284

Nishioka, S.; Takeda, C.S.; Wong, W.K. Johnson, Size-fractionated iron concentrations in the northeast Pacific Ocean: distribution of soluble and small colloidal iron Mar. Chem., 2001; 74: 157-179

Pelizzetti, E.; Minero, C.; Maurino, V. The role of colloidal particles in the photodegradation of organic compounds of environmental concern in aquatic systems Adv. Colloid. Interf. Sci. 1990; 32: 271-316

Petasne, R.G.; Zika, R.G. Fate of superoxide in coastal sea water. Nature 1987; 325: 516-518

Rose, L.; Waite, T.D. Kinetic model for Fe(II) oxidation in seawater in the absence and presence of natural organic matter. Environ. Sci. Technol. 2002; 36: 433-444

Santana-Casiano, J.M.; Gonzalez-Davila, M.; Millero, F.J. Oxidation of Fe(II) with oxygen in natural waters. Environ. Sci. Technol. 2005; 39: 2073-2079

Santana-Casiano, J.M.; Gonzalez-Davila, M.; Millero, F.J. The role of Fe(II) species on the oxidation of Fe(II) in natural waters in the presence of $O_2$ and $H_2O_2$. Mar. Chem. 2006; 99: 70-82

Sarthou, G.; Jeandel, C.; Seasonal variations of iron concentrations in the Ligurian Sea and iron budget in the Western Mediterranean Sea Mar.Chem. 2001**;** 74: 115-129

Spokes, L.J.; Liss, P.S. Photochemically induced redox reactions in seawater. Cations Mar. Chem., 1995; 49: 201-213

Stumm, W.; Sulzberger, B. The cycling of iron in natural environments: considerations based on laboratory studies of heterogeneous redox processes. Geochim. Cosmochim. Acta 1992; 56: 3233-3257

Vione, D.; Maurino, V.; Man, S.C., Khanra, S.; Arsene, C.; Olariu, R.I.; Minero, C., Formation of organobrominated compounds in the presence of bromide under simulated atmospheric aerosol conditions, Chem. Sus. Chem. 2008; 1: 197-204

Wu, J.; Boyle, E.; Sunda, W.; Wen, L.S., Soluble and colloidal iron in the oligotrophic North Atlantic and North Pacific, Science, 2001; 293: 847-849

Yao, W.; Millero, F.J., The chemistry of the anoxic waters in the Framvaren Fjord Norway, Aquat. Geochem. 1995; 1: 53-88

## Figure caption

**Fig. 1.** Hydrogen peroxide formation as a function irradiation time (unstirred and filtered solution) in the presence of phenol $2x10^{-4}$ M: (A) added with Fe(II) [$1x10^{-4}$M] in ASW and NaCl 0.7 M; (B) added with Fe(III) [$1x10^{-4}$ M] in ASW, and at pH 8 with or without NaCl 0.7 M.

**Fig. 2.** Intermediate compounds formed during phenol photo-transformation in ASW added with goethite 200 $mgL^{-1}$: (A) hydroxyl and condensed products; (B) halogenated products.

**Fig. 3**. Intermediate compounds formed during phenol photo-transformation in ASW added with akaganeite 200 $mgL^{-1}$: (A) hydroxyl and condensed products; (B) halogenated products.

**Fig. 4** Maximal concentration of intermediate compounds formed during phenol photo-transformation in ASW spiked with akaganeite, hematite, goethite, Fe(II) or Fe(III). Compounds are ordered as (top) hydroxylated (resorcinol, hydroquinone, 1,4-benzoquinone), condensed (2,2'-bisphenol, 2,4'-bisphenol 4,4'-bisphenol, 4-phenoxyphenol, 2-phenoxyphenol), nitrated (2-nitrophenol, 4-nitrophenol) and (bottom) halogenated (2-chlorophenol, 3-chlorophenol, 4-chlorophenol, 2,3-dichlorophenol, 2,4-dichlorophenol 3,4-dichlorophenol, 2,6-dichlorophenol, 2,4,6-trichlorophenol, 2-bromophenol and 4-bromophenol)

**Fig. 5** Maximal concentration of intermediate compounds formed during phenol photo-transformation in natural seawater (NSW) spiked with akaganeite, goethite, Fe(II), Fe(III). Compounds are ordered as (top) hydroxylated (resorcinol, hydroquinone, 1,4-benzoquinone), condensed (2,2'-bisphenol, 2,4'-bisphenol 4,4'-bisphenol, 4-phenoxyphenol, 2-phenoxyphenol), nitrated (2-nitrophenol, 4-nitrophenol) and (bottom) halogenated (2-chlorophenol, 3-chlorophenol, 4-chlorophenol, 2,3-dichlorophenol, 2,4-dichlorophenol 3,4-dichlorophenol, 2,6-dichlorophenol, 2,4,6-trichlorophenol, 2-bromophenol and 4-bromophenol)

Figure 1

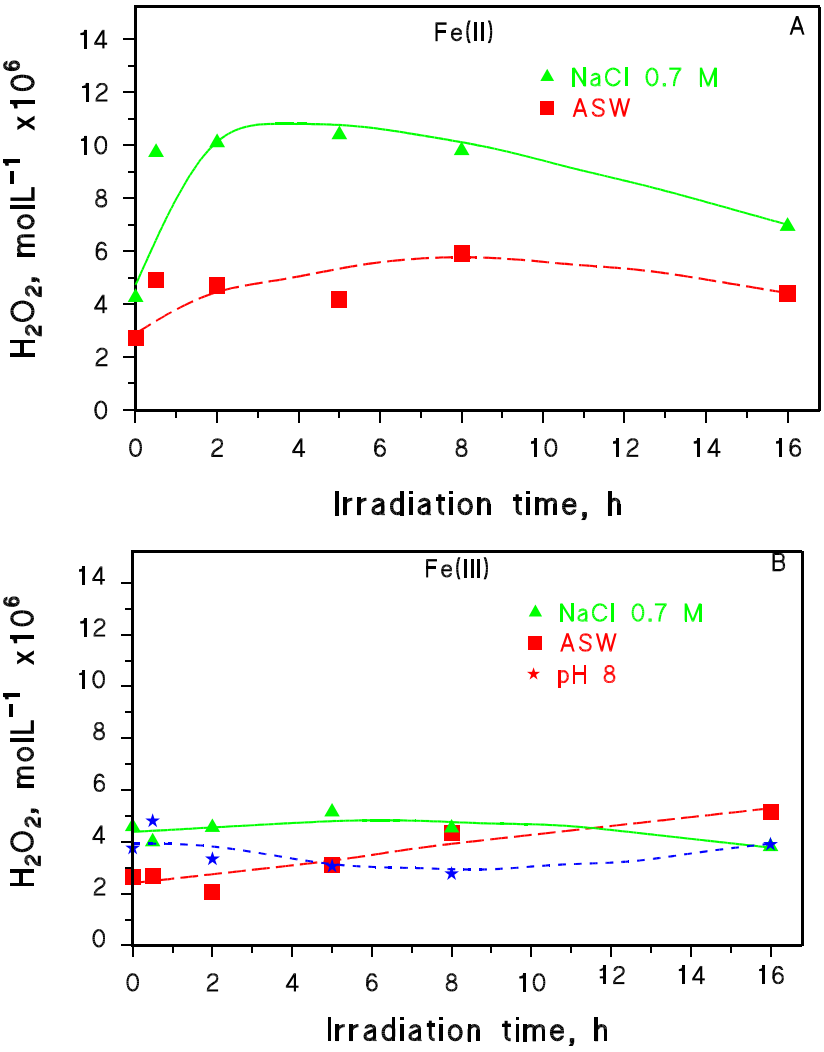
Fe(II)
A
NaCl 0.7 M
ASW
$H_2O_2$, molL$^{-1}$ x10$^6$
Irradiation time, h
Fe(III)
B
NaCl 0.7 M
ASW
pH 8
$H_2O_2$, molL$^{-1}$ x10$^6$
Irradiation time, h

Figure 2

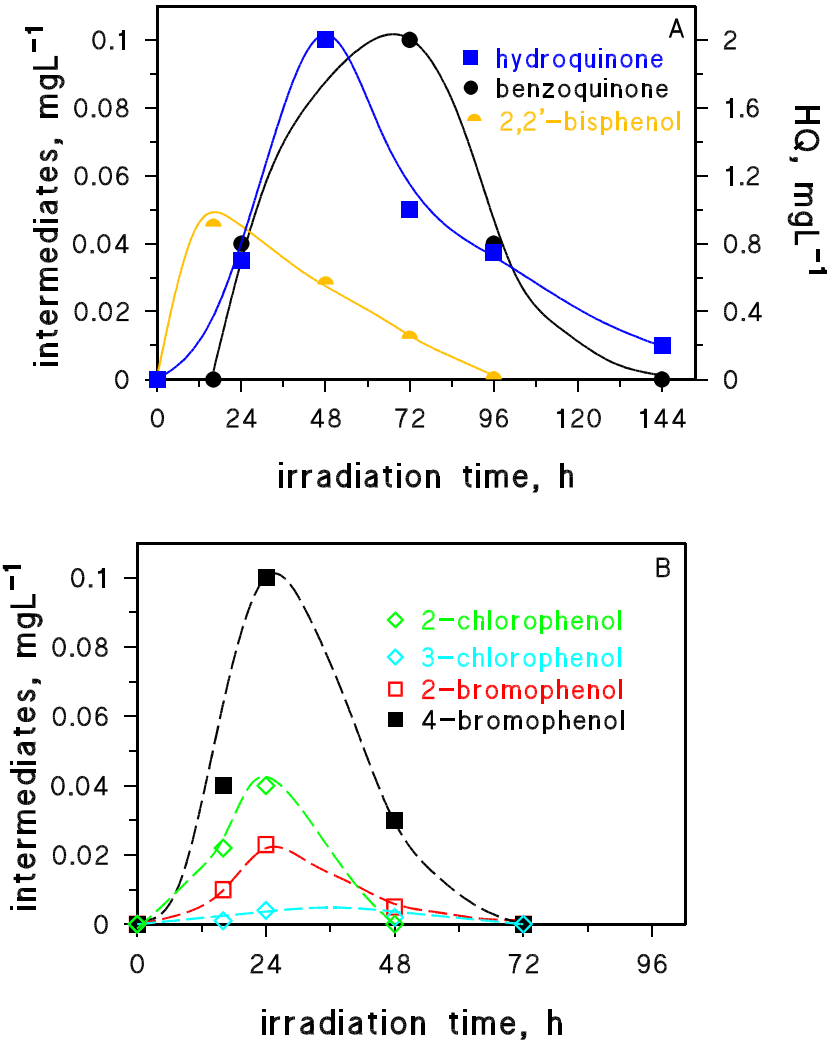
A
hydroquinone
benzoquinone
2,2'–bisphenol
intermediates, mgL⁻¹
HQ, mgL⁻¹
irradiation time, h
B
2–chlorophenol
3–chlorophenol
2–bromophenol
4–bromophenol
intermediates, mgL⁻¹
irradiation time, h

Figure 3

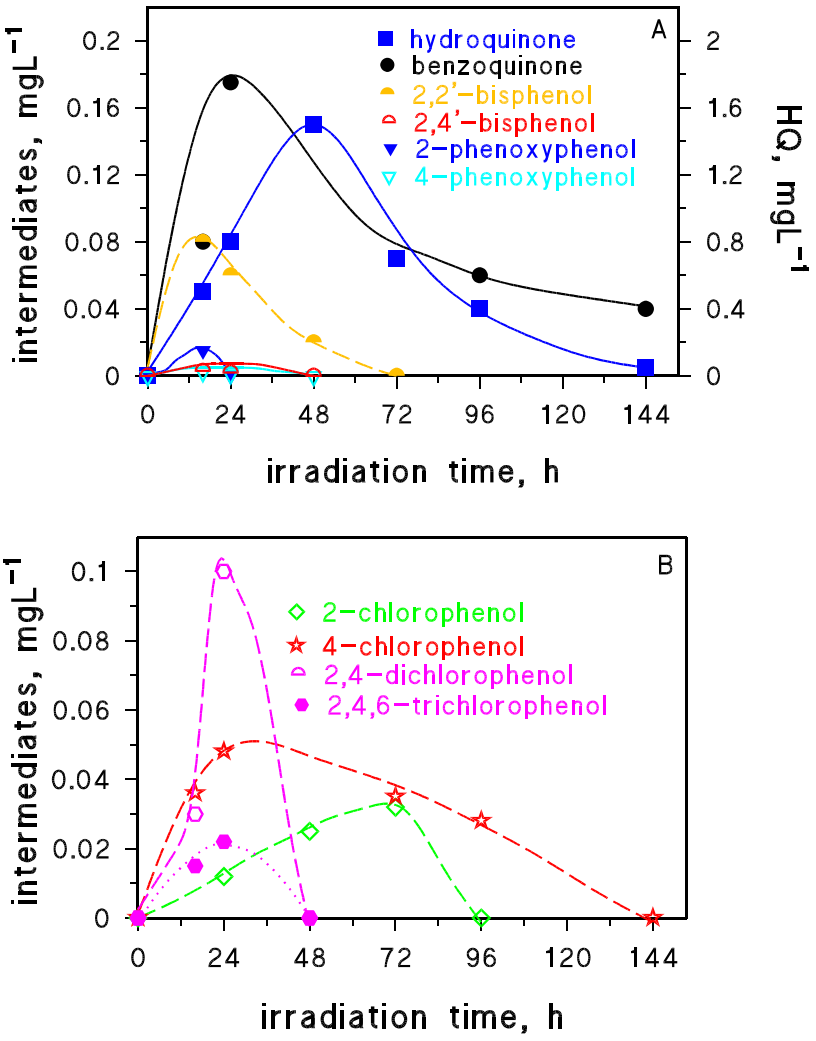
A
hydroquinone
benzoquinone
2,2'–bisphenol
2,4'–bisphenol
2–phenoxyphenol
4–phenoxyphenol
intermediates, mgL-1
HQ, mgL-1
irradiation time, h
B
2–chlorophenol
4–chlorophenol
2,4–dichlorophenol
2,4,6–trichlorophenol
intermediates, mgL-1
irradiation time, h

Figure 4

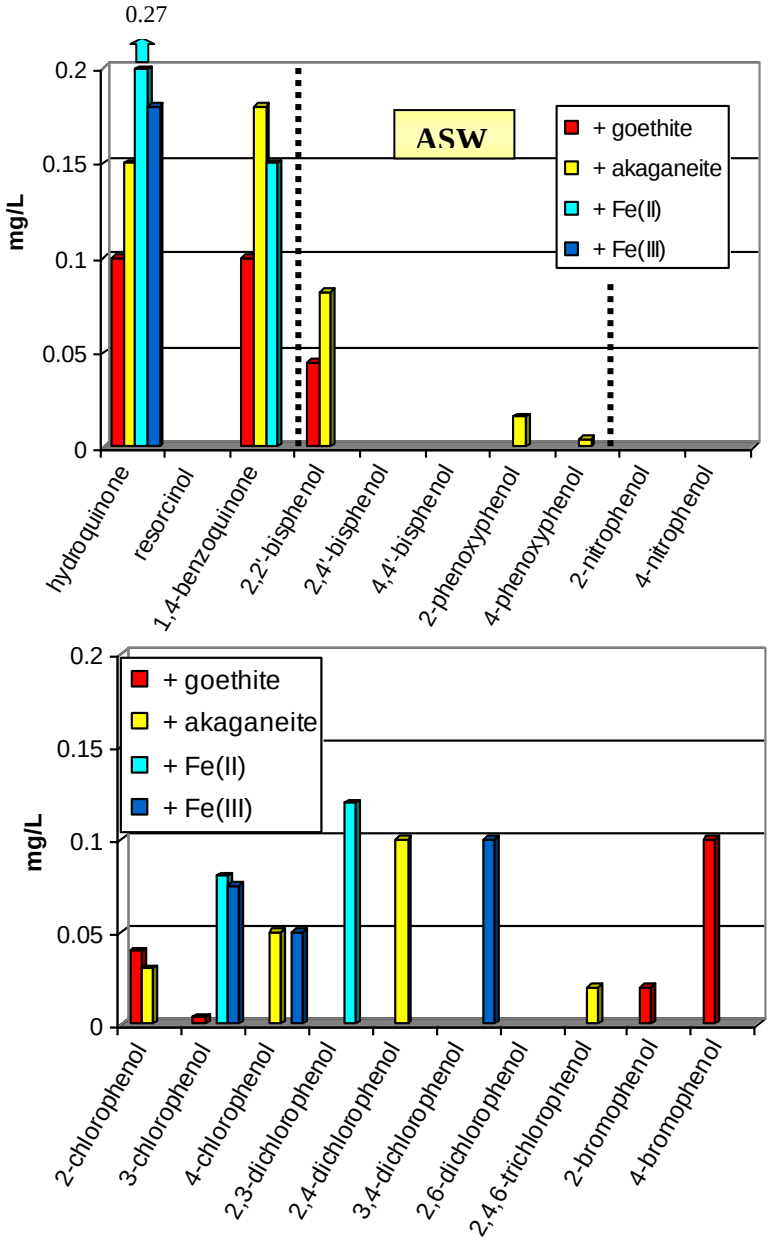
0.27
0.2
0.15
0.1
0.05
0
mg/L
ASW
+ goethite
+ akaganeite
+ Fe(II)
+ Fe(III)
hydroquinone
resorcinol
1,4-benzoquinone
2,2'-bisphenol
2,4'-bisphenol
4,4'-bisphenol
2-phenoxyphenol
4-phenoxyphenol
2-nitrophenol
4-nitrophenol
0.2
0.15
0.1
0.05
0
mg/L
+ goethite
+ akaganeite
+ Fe(II)
+ Fe(III)
2-chlorophenol
3-chlorophenol
4-chlorophenol
2,3-dichlorophenol
2,4-dichlorophenol
3,4-dichlorophenol
2,6-dichlorophenol
2,4,6-trichlorophenol
2-bromophenol
4-bromophenol

Figure 5

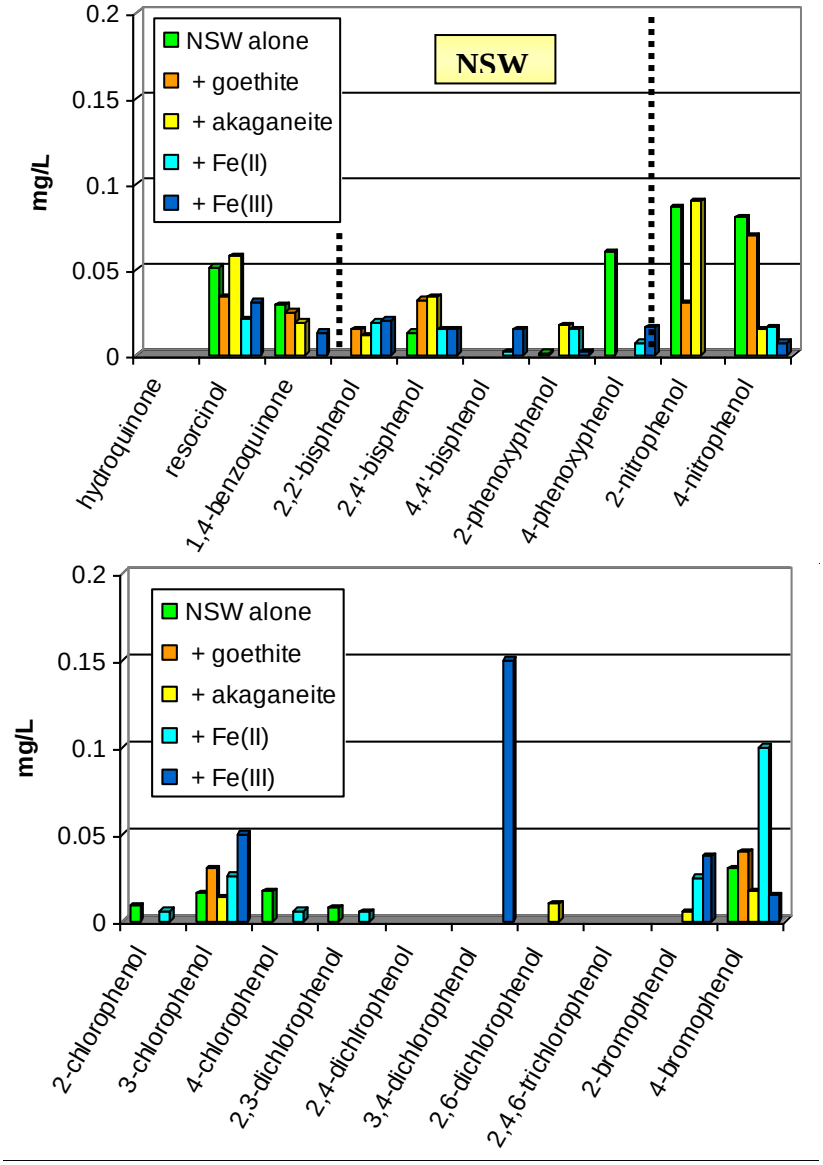
NSW
NSW alone
+ goethite
+ akaganeite
+ Fe(II)
+ Fe(III)
mg/L
0.2
0.15
0.1
0.05
0
hydroquinone
resorcinol
1,4-benzoquinone
2,2'-bisphenol
2,4'-bisphenol
4,4'-bisphenol
2-phenoxyphenol
4-phenoxyphenol
2-nitrophenol
4-nitrophenol
2-chlorophenol
3-chlorophenol
4-chlorophenol
2,3-dichlorophenol
2,4-dichlorophenol
3,4-dichlorophenol
2,6-dichlorophenol
2,4,6-trichlorophenol
2-bromophenol
4-bromophenol

**Table 1**. Main components in different media: NaCl solution, artificial seawater (ASW), natural seawater (NSW).

| | **NaCl** | **ASW** | **NSW** |
|---|---|---|---|
| **salinity** | 39.90 | 35.00 | 36.06 |
| **pH** | 7.98 | 8.03 | 8.21 |
| **N-$NH_3$** | - | - | 0.90 μmol $dm^{-3}$ |
| **N-$NO_2$** | - | - | 0.28 μmol $dm^{-3}$ |
| **N-$NO_3$** | - | - | 4.67 μmol $dm^{-3}$ |
| **Fe** | - | - | 49,4 μg/L |
| **DOM** | - | - | 18.7 $mgL^{-1}$ |

**Table 2**. Artificial seawater composition.

| **Salt** | **g/Kg** | **Purity** | **Supplier** |
|---|---|---|---|
| NaCl | 23.9849 | 99.5% | Fluka |
| $Na_2SO_4$ | 4.0111 | 99% | Aldrich |
| KCl | 0.6926 | 99.7% | Aldrich |
| $NaHCO_3$ | 0.1722 | 99.5% | Aldrich |
| KBr | 0.1 | 99% | Fluka |
| $B(OH)_3$ | 0.0254 | 99% | Aldrich |
| NaF | 0.0029 | 99% | Merck |
| $MgCl_2$ | 5.0290 | 99% | Carlo Erba |
| $CaCl_2$ | 1.1409 | 98% | Aldrich |
| $SrCl_2$ | 0.0143 | 99% | Carlo Erba |

**Table 3.** Initial rate for the disappearance of phenol $2x10^{-4}$ M at pH 8 under different media; added with iron oxides, Fe(II) [$1x10^{-4}$M] and Fe(III) [$1x10^{-4}$M]. Conditions: stirred (**S**, for 96h) or unstirred (**US**, no equilibration time) solution, filtered (**F**, 0.45 μm) or unfiltered (**UF**) solution.

| **Rate, $Mmin^{-1}$ $x10^7$** | **NaCl 0.7 M** | | | | **ASW** | | | | **NSW** |
|---|---|---|---|---|---|---|---|---|---|
| | **S/UF** | **S/ F** | **US/UF** | **US/F** | **S/UF** | **S/ F** | **US/UF** | **US/F** | **US/UF** |
| **Fe(II)** | 11.2±0.1 | 11.0±0.2 | 12.2±0.1 | 11.8±0.2 | 10.2±0.2 | 10.4±0.3 | 8.2±0.1 | 8.8±0.2 | 26.4±0.3 |
| **Fe(III)** | 9.8±0.1 | 9.5±0.22 | 10.2±0.2 | 10.0±0.2 | 8.6±0.1 | 8.4±0.2 | 8.4±0.2 | 8.2±0.1 | 24.6±0.2 |

| | | | |
|---|---|---|---|
| **Akaganeite** | 25 ±0.2 | 23.6±0.1 | 32.2±0.3 |
| **Goethite** | 14.4±0.1 | 11.4±0.1 | 28.6±0.2 |